ELSEVIER

International Journal of Mass Spectrometry 218 (2002) 1–10

International Journal of Mass Spectrometry

www.elsevier.com/locate/ijms

Ion rearrangement at the beginning of cluster formation: isomerization pathways and dissociation kinetics for the ionized dimethylamine dimer

Paul M. Mayer

Department of Chemistry, University of Ottawa, Ottawa, Canada K1N 6N5

Received 20 December 2001; accepted 13 March 2002

Abstract

Density functional theory (B3-LYP/6-311++G(3df,2p)//B3-LYP/6-31+G(d)) is used to explore the unimolecular reaction chemistry of ionized dimethylamine dimers. Three stable isomers were found to exist on the surface, one retaining the connectivity of the neutral dimer of dimethylamine and two resulting from a hydrogen shift in the dimer ion forming complexes between protonated dimethylamine and the $CH_3NHCH_2^{\bullet}$ free radical. The barriers for their interconversion suggest that ionization of neutral dimethylamine dimers results in ions retaining the original connectivity, but that they undergo rapid equilibration with one of the isomers. The dissociation kinetics of the dimethylamine dimer ions have been estimated by RRKM theory using both two- and three-well potential models for the reaction. Agreement between the predicted observed rate constant based on the B3-LYP/6-311++G(3df,2p)//B3-LYP/6-31+G(d) surface and recent TPEPICO results for this system are excellent. (Int J Mass Spectrom 218 (2002) 1–10)

Keywords: RRKM; Density functional theory; Unimolecular decomposition; Cluster ion

1. Introduction

The study of clusters of organic and inorganic molecules has seen a dramatic growth over the last 20 years. Clusters of molecules can be viewed as an intermediate state of matter between the dilute gas phase and solution and studying them allows the effects of solvation on the chemistry of gas-phase molecules and ions to be explored [1–5]. Ionic clusters (typically made up of a core ion surrounded by one or more solvating molecules) are known to be involved in the chemistry of the upper and mid atmosphere [6].

A central issue when studying the chemistry of gaseous ions is their propensity for rearrangement prior to reaction. Over the years a variety of thermodynamically stable structures such as distonic ions, ion–neutral complexes and bridged ions have been discovered that have key roles in ion dissociation mechanisms. The isomerization of more conventional organic ions is well known and appears to be a common occurrence, though the isomerization reactions of cluster ions have not been as extensively studied (for examples, see [4,7–17]). A recent report by Mayer et al. [11] describing the unimolecular chemistry of the ionized dimer of dimethylamine is such an example. Ionized dimers of dimethylamine dissociate to form protonated dimethylamine and a free radical.

E-mail: pmayer@science.uottawa.ca

1387-3806/02/$ – see front matter
PII S1387-3806(02)00640-1

Threshold photoelectron-photoion coincidence (TPEPICO) measurements of the unimolecular dissociation rate constant of the ionized dimer were modeled to extract the dimer ion binding energy. Ab initio calculations at the MP2/6-31G(d) level of theory performed at the time concluded that the dimer ion geometry consisted of protonated dimethylamine hydrogen bonded to the carbon atom in the $CH_3NHCH_2^{\bullet}$ free radical. The experimental activation energy for the dimer ion dissociation, 0.99 ± 0.03 eV (96 ± 3 kJ mol^{-1}) was derived from a variational RRKM fit to the experimental rate constant vs. internal energy data. The MP2/6-31G(d) calculations estimated the activation energy for the dissociation of this ion to form $(CH_3)NH_2^+ + CH_3NHCH_2^{\bullet}$ to be 81 kJ mol^{-1}. In light of this discrepancy, it is possible that the theoretical model for the reaction was incomplete, and that the dissociation takes place via an alternative process. In the present theoretical study, thermodynamically stable isomers of the dimethylamine dimer ion are located on the potential energy surface and their interconversion is explored. The results are viewed in light of the TPEPICO measurements previously made for the dimer ion.

2. Computational details

Standard density functional theory calculations [18] were performed using the Gaussian 98 [19] suite of programs. Geometry optimizations and vibrational frequencies (scaled by 0.96 [20]) were obtained at the B3-LYP/6-31+G(d) level of theory. A recent assessment of theoretical procedures for describing open-shell systems [21] concluded that the B3-LYP level of theory provided reasonable geometries and relative energies. A series of theoretical assessments [22–24] of proton-bound dimers involving HCN and CH_3CN with a variety of first-row hydrides has shown that geometries optimized at the B3-LYP/6-31+G(d) level of theory provide an adequate foundation for high level single-point energy calculations and that relative energies obtained at this level are usually close to those obtained with more sophisticated theories such as G2 theory. The average error between B3-LYP/6-31+G(d) and G2 values for four nitrile-containing proton-bound dimers was found to be ± 3 kJ mol^{-1} [24]. Single-point energy calculations on the B3-LYP/6-31+G(d) geometries were also carried out at the B3-LYP/6-311++G(3df,2p) level of theory. The average error for this level of theory (as compared to G2 theory) for proton-bound pairs containing a nitrile should be similar to that found for the B3-LYP/6-311+G(2df,p)//B3-LYP/6-31+G(d) level of theory, ± 4 kJ mol^{-1} [24]. However, there may be greater uncertainty for transition state energies and for isomeric structures that are not proton-bound pairs. It is difficult to estimate the uncertainty in those values. Transition states were confirmed by the intrinsic reaction coordinate procedure in Gaussian 98.

3. Results and discussion

3.1. Calculated minimum energy reaction pathways

Three thermodynamically and kinetically stable isomers of the dimethylamine dimer ion were identified at the B3-LYP/6-31+G(d) level of theory. Optimized geometries for the neutral dimethylamine dimer and the three isomeric dimer ions can be found in Fig. 1. The neutral dimer **1n** features a hydrogen bond between the two nitrogen atoms, and corresponds to that obtained at the MP2/6-31G(d) level of theory by Mayer et al. [11]. The geometry is consistent with experimental data for the dimer from microwave spectroscopy obtained by Tubergen and Kuczkowski [25]. All of the ionic forms of the dimer can be described as complexes between protonated dimethylamine, $(CH_3)_2NH_2^+$, and a free radical. Ion **1** is most closely related to the neutral structure though the $(CH_3)_2N^{\bullet}$ radical is twisted 90° relative to the protonated moiety. Ions **2** and **3** are both complexes between protonated dimethylamine and a carbon-centered free radical, $CH_3NHCH_2^{\bullet}$, with **3** exhibiting a hydrogen bond to nitrogen and **2** having the hydrogen bond to the radical center. This latter structure was reported previously by Mayer et al. [11]. The relative energies of these three isomers

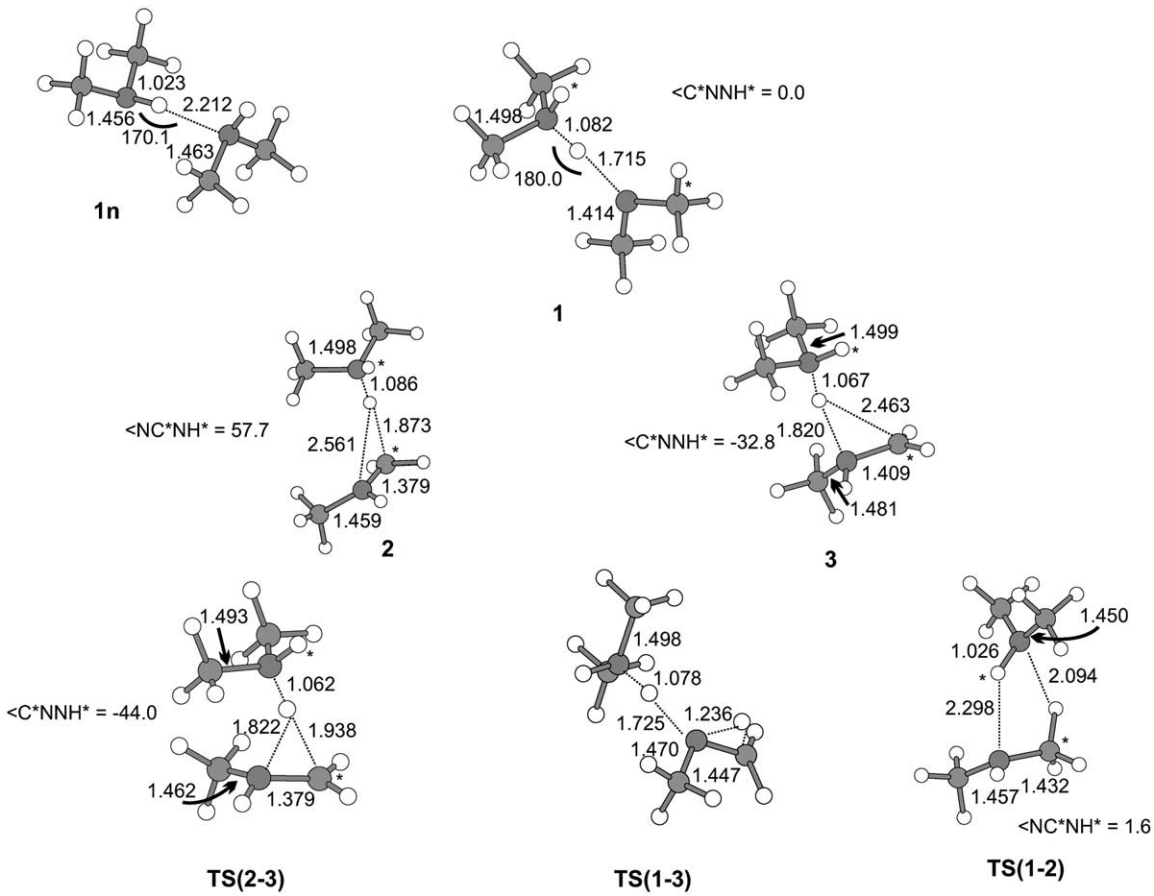

Fig. 1. Optimized geometries of equilibrium and transition state species obtained at the B3-LYP/6-31+G(d) level of theory. Bond lengths are in Angstrom and angles in degrees. Selected dihedral angles are presented as ∠ABCD, with atoms labeled by an asterisk (*) used to aid in the interpretation.

can be found in Table 1 along with the various possible dissociation products and the energy of the vertical structure of the ion. The ion having the same structure as the neutral dimer (vertical structure, **1v**) has a relative energy below that of the dissociation products.

Knowledge of the possible equilibrium species present on the potential energy surface is important, but it is also important to consider the isomerization barriers between these species. Transition structures were found connecting ions **1** and **2** (**TS1-2**) and ions **2** and **3** (**TS2-3**) and ions **1** and **3** (**TS1-3**) (Fig. 2). Transition structure **TS1-3** involves the interconversion of ions **1** and **3** via a 1,2-hydrogen shift and predictably lies very high in energy. Ions **2** and **3** interconvert by the migration of protonated dimethylamine from carbon to nitrogen in the free radical and the interconversion of ions **1** and **2** occurs via a five-member transition state (**TS1-2**), both processes lying below the dissociation thresholds.

3.2. Unimolecular dissociation kinetics modeling

The potential energy surface in Fig. 2 can be modeled with RRKM theory to predict the unimolecular decay rate for ionized dimethylamine dimers. A simplified model, ignoring the reactions of ion **3** will be

Table 1
Calculated relative energies for equilibrium, transition state and dissociation product structures

	B3-LYP/	
	6-31+G(d)	6-311++G(3df,2p)
1	0	0
2	27	16
3	33	24
Vertical (**1v**)	81	85
TS(1-3)	192	180
TS(2-3)	89	75
TS(1-2)	53	49
$(CH_3)_2NH_2^+ + (CH_3)_2N^\bullet$	94	92
$(CH_3)_2NH_2^+ + CH_3NHCH_2^\bullet$	101	87
$(CH_3)_2NH^{\bullet+} + (CH_3)_2NH$	117	110

In kJ mol^{-1} at 0 K.

developed followed by a complete treatment involving all three equilibrium species. In each case the results are compared to the experimental $k(E)$ vs. E data obtained for the dissociation of the dimethylamine dimer ions obtained by Mayer et al. [11] with TPEPICO spectroscopy. The RRKM evaluation of the rate constants for the elementary reactions in Fig. 2 employed the B3-LYP/6-311++G(3df,2p)//B3-LYP/6-31+G(d) relative energies in Table 1 and the scaled B3-LYP/6-31+G(d) vibrational frequencies (Table 2). For isomerization reactions, the standard RRKM expression was employed:

$$k(E) = \frac{\sigma N^{\ddagger}(E - E_0)}{h\rho(E)}$$

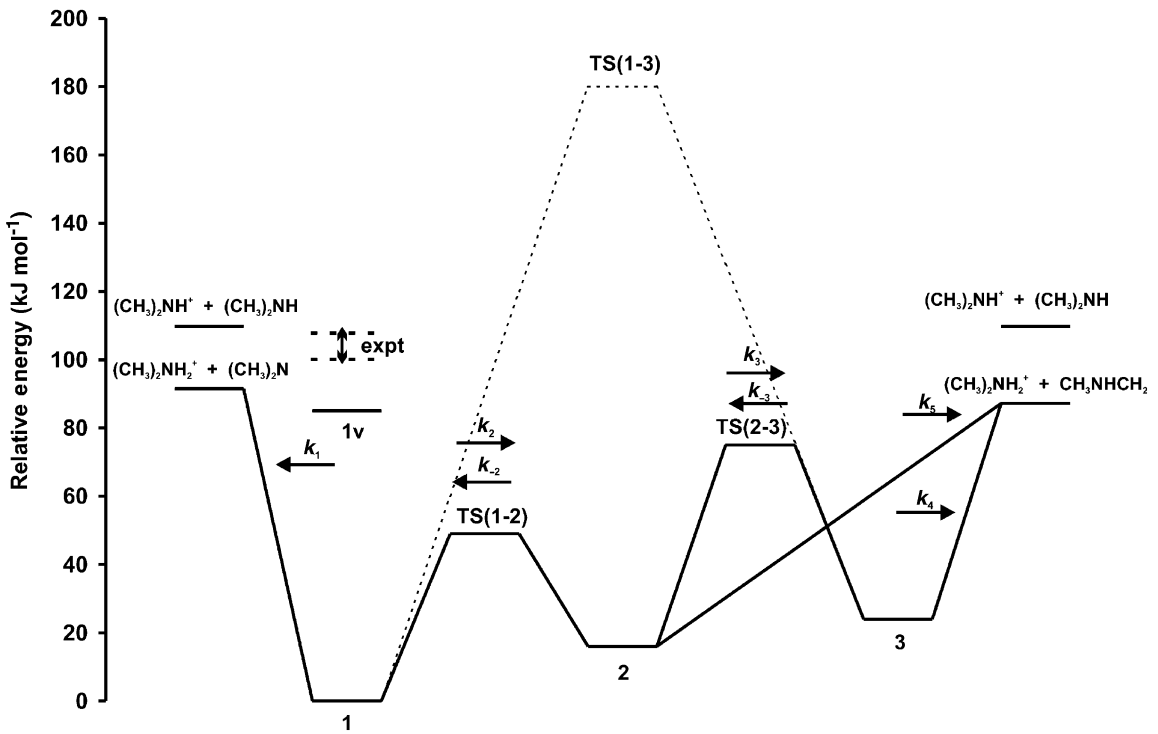

Fig. 2. B3-LYP/6-311++G(3df,2p)//B3-LYP/6-31+G(d) minimum energy reaction pathway surface for the isomerization and dissociation of ionized dimethylamine dimers. The dashed lines represent the internal energy range spanned by the TPEPICO data obtained by Mayer et al. [11].

Table 2
Harmonic vibrational frequencies used in the RRKM analysis

1			**2**			**3**			**TS(1-2)**			**TS(2-3)**			**TS(1-Pdts)**			**TS(3-Pdts)**			**TS(2-Pdts)**	
18[a]	44	75	8[b]	56	88	28[c]	75	81	(236)	50	66	(288)	48	117	(2459)	18[a]	1491	(2683)	28[c]	3131	(2363)	8[b]	3129
79	102	145	115	133	144	150	168	187	92	116	135	146	177	206	36	1005	1495	67	3035	3390	47	3034	3391
194	195	238	186	212	290	192	243	279	163	201	250	232	293	319	62	1035	1498	72	3089	279	73	3061	290
303	383	452	354	383	473	289	383	391	277	380	402	348	390	394	62	1081	1549	129	3129	391	117	3127	473
862	909	915	554	860	878	402	841	862	505	736	894	440	636	796	85	1194	1727	162	3251	862	109	3162	878
968	1002	1003	885	940	1002	878	910	1000	917	1027	1038	872	932	1007	116	1212	2934	123	243	1000	94	212	1002
1005	1035	1081	1030	1050	1079	1022	1032	1082	1044	1073	1113	1018	1033	1075	194	1227	2942	192	383	1082	186	383	1079
1194	1212	1227	1113	1225	1236	1131	1183	1227	1124	1139	1166	1128	1204	1230	195	1264	2981	231	841	1227	354	860	1236
1264	1387	1408	1256	1302	1405	1250	1258	1408	1236	1237	1416	1253	1292	1401	238	1387	2989	402	910	1408	554	940	1405
1410	1431	1450	1429	1434	1452	1428	1431	1449	1432	1433	1439	1429	1438	1443	303	1408	3034	878	1032	1449	885	1050	1452
1455	1462	1474	1458	1471	1478	1457	1472	1475	1445	1448	1457	1453	1467	1480	383	1410	3036	1022	1183	1475	1030	1225	1478
1475	1486	1491	1483	1486	1494	1484	1486	1495	1461	1465	1472	1482	1487	1496	452	1431	3073	1131	1258	1495	1113	1302	1494
1495	1498	1549	1496	1513	1531	1497	1508	1551	1477	1484	1497	1504	1515	1539	862	1450	3076	1250	1431	1551	1256	1434	1531
1727	2459	2934	1655	2363	2983	1695	2683	2996	1504	2635	2942	1630	2855	3005	909	1455	3125	1428	1472	2996	1429	1471	2983
2942	2981	2989	3034	3036	3050	3035	3037	3066	2950	2961	2993	3048	3053	3075	915	1462	3125	1457	1486	3066	1458	1486	3050
3034	3036	3073	3061	3089	3125	3089	3127	3127	3024	3045	3051	3101	3107	3138	968	1474	3128	1484	1508	3127	1483	1513	3125
3076	3125	3125	3127	3129	3130	3129	3131	3131	3062	3078	3090	3141	3147	3154	1002	1475	3128	1497	3037	3131	1496	3036	3130
3128	3128	3393	3162	3391	3517	3251	3390	3425	3116	3305	3500	3200	3369	3481	1003	1486	3393	1695	3127	3425	1655	3089	3517

Values in cm^{-1}. Imaginary modes in the transition states are in parentheses.

[a] Mode replaced by an internal rotation with constant 4.4 GHz in simple bond cleavage reaction.

[b] Mode replaced by an internal rotation with constant 5.2 GHz in simple bond cleavage reaction.

[c] Mode replaced by an internal rotation with constant 4.3 GHz in simple bond cleavage reaction.

where $N^{\ddagger}(E-E_0)$ is the transition state sum-of-states above the activation energy E_0 and $\rho(E)$ is the density of states of the reactant ion at an internal energy E. The sums and densities of states were obtained via the direct count algorithm of Beyer and Swinehart [26]. The only unknowns are the effective transition states for the three simple bond cleavage reactions governed by k_1, k_4 and k_5 (Fig. 2). The previous variational RRKM treatment [11] derived an entropy of activation, $\Delta S^{\ddagger}$ (600 K), for the dissociation of ion **2** of $8\,\mathrm{J\,K^{-1}\,mol^{-1}}$, and so in the present study the transition state vibrational frequencies for the three simple cleavage reactions were estimated by employing the vibrational frequencies of the reactant ions and scaling the lowest five modes to achieve this $\Delta S^{\ddagger}$. In addition, the vibration in the reactant ion due to rotation about the hydrogen bond was removed from both the reactant ion and approximated transition state and was treated as a hindered internal rotation [27]. The rate constants for the seven elementary reactions of interest in Fig. 2 are listed in Table 3 and plotted in Fig. 3 as a function of the internal energy of ion **1**.

3.2.1. Two-well, three product channels

In a simplified model that ignores reactions of ion **3**, the experimentally observed dissociation rate constant, k_{obs}, can be related to the individual rate constants shown in Fig. 3. Baer et al. solved the two-well model [28] and it has successfully been extended to systems involving more than two products [29,30]. The rate of production of products (let P_1 be $(CH_3)_2NH_2^+ + (CH_3)_2N^{\bullet}$ and P_2 be $(CH_3)_2NH_2^+ + CH_3NHCH_2^{\bullet}$) is:

$$\frac{\mathrm{d}[P_1]}{\mathrm{d}t} = k_1[\mathbf{1}], \qquad \frac{\mathrm{d}[P_2]}{\mathrm{d}t} = k_5[\mathbf{2}]$$

The rate of change in concentration for ion **1** and **2** can be written as:

$$\frac{\mathrm{d}[\mathbf{1}]}{\mathrm{d}t} = (-k_1 - k_2)[\mathbf{1}] + k_{-2}[\mathbf{2}] = a_1[\mathbf{1}] + b_1[\mathbf{2}],$$

$$\frac{\mathrm{d}[\mathbf{2}]}{\mathrm{d}t} = k_2[\mathbf{1}] + (-k_{-2} - k_5 - k_3)[\mathbf{2}] = a_2[\mathbf{1}] + b_2[\mathbf{2}]$$

Table 3
RRKM rate constants used in the two- and three-well potential models

E^{a}	k_1	k_2	k_{-2}	k_3	k_{-3}	k_4	k_5
0.950	1	39595579	769774310	31737	798346	17610	4439
0.963	8	44124499	838262600	41213	1021700	39953	10478
0.976	45	49012692	910336310	52593	1284582	80191	21733
0.989	160	54275902	986041740	66368	1598486	149521	41248
1.003	436	59930128	1065426500	82597	1962301	259582	72684
1.016	1023	65991241	1148531800	101646	2381915	426542	121065
1.029	2148	72475274	1235398400	123910	2865992	670638	192027
1.042	4130	79398107	1326061700	149540	3414628	1013966	292875
1.055	7409	86775751	1420556900	179111	4038041	1483987	431575
1.068	12557	94624111	1518915100	212889	4741312	2111391	618055
1.081	20290	102959060	1621165100	251159	5526534	2930497	862925
1.095	31494	111796480	1727333800	294528	6404234	3981282	1178988
1.108	47242	121152160	1837445600	343201	7377501	5307259	1579990
1.121	68803	131041840	1951523200	397660	8451718	6956840	2082102
1.134	97678	141481170	2069586400	458472	9636342	8984664	2702684
1.147	135617	152485770	2191654100	525890	10934627	11449290	3461684
1.160	184654	164071080	2317742200	600500	12353299	14415252	4380607
1.173	247136	176252540	2447865700	682772	13899634	17954064	5483633
1.187	325751	189045370	2582036800	773073	15578296	22141499	6796791
1.200	423572	202464740	2720266700	872049	17396612	27060124	8348819

All values in s^{-1}.

[a] Internal energy of ion **1** (eV).

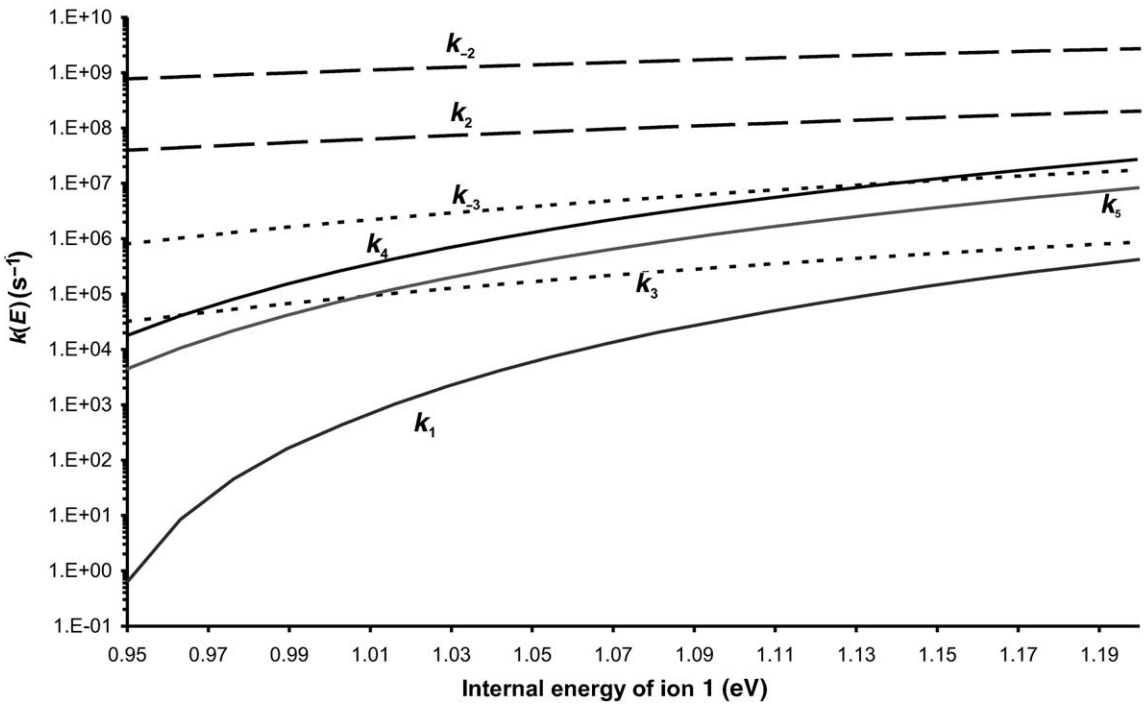

Fig. 3. Logarithmic plot of $k(E)$ vs. the internal energy of ion **1** for the seven rate constants shown in Fig. 2.

General solutions are of the form:

$$[\mathbf{1}] = c_1\alpha_1 \, e^{-\lambda_1 t} + c_2\alpha_2 \, e^{-\lambda_2 t},$$
$$[\mathbf{2}] = c_1\beta_1 \, e^{-\lambda_1 t} + c_2\beta_2 \, e^{-\lambda_2 t}$$

where λ are the eigenvalues of the matrix:

$$\begin{bmatrix} \lambda + a_1 & b_1 \\ a_2 & \lambda + b_2 \end{bmatrix} \begin{pmatrix} \alpha \\ \beta \end{pmatrix} = \begin{pmatrix} 0 \\ 0 \end{pmatrix}$$

the α's and β's are the eigenvectors and c_1 and c_2 are constants. This matrix can be solved numerically if values for k_1 to k_5 are available (Table 3). Baer et al. solved for the eigenvalues and eigenvectors algebraically for a few limiting cases [28]. The large magnitudes of k_2 and k_{-2} relative to the other rate constants means that ions **1** and **2** rapidly interconvert prior to further reaction. Thus, a two-well model accounting for the "equilibration" of reactant ion structures prior to dissociation is needed [28]. The final observed rate in this situation has a fast component and a slow component. The fast component only contributes to the product ion flux near $t = 0$, and so both products are observed to be formed with a single exponential rate. The rate constant in terms of $k_1 - k_5$ for this observed channel is [28]:

$$k_{\text{obs}} = \frac{k_1 k_{-2}}{k_2} + k_5$$

If the isomerization from **2** to **3** is added as a second product channel for ion **2** the expression becomes [29]:

$$k_{\text{obs}} = \frac{k_1 k_{-2}}{k_2} + k_3 + k_5$$

Based on the photon energy for each experimental data point and the B3-LYP/6-311++G(3df,2p)//B3-LYP/6-31+G(d) adiabatic ionization energy of the neutral dimer **1n**, 7.08 eV, the experimental data of Mayer et al. [11] lies between 1.04 and 1.12 eV internal energy of ion **1**. A plot of k_{obs} vs. the internal energy of ion **1** is shown in Fig. 4 and, even for this approximate model, is in excellent agreement with the TPEPICO

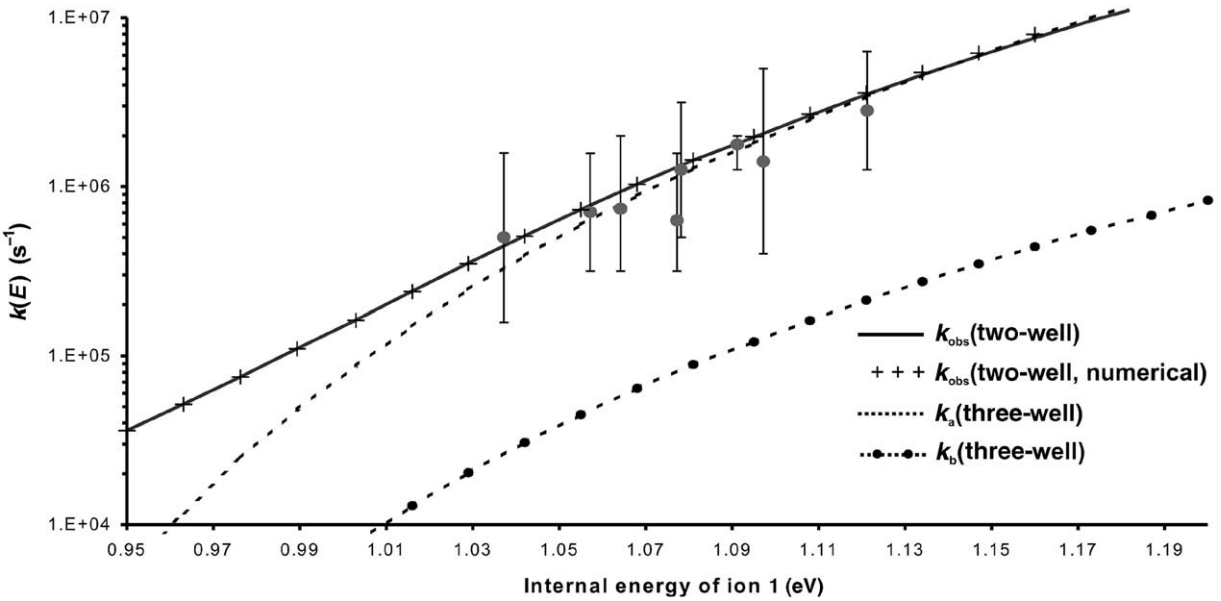

Fig. 4. Plot of k_{obs} for a two-well potential model incorporating the rapid interconversion of ions **1** and **2** prior to their dissociation, based on numerical evaluation and the approximate solution developed by Baer et al. [28]. Plot of k_a and k_b for the numerical evaluation of the three-well model. The experimental data and error limits were taken from [11].

data. This indicates that the formation of products via ion **3** is small over the internal energy range probed in the TPEPICO experiment. Also shown in Fig. 4 is the result of the numerical evaluation of the eigenvectors of the matrix with no assumptions concerning the relative values of the individual rate constants. Agreement with Baer et al.'s approximate treatment is again excellent.

3.2.2. Three-well, three product channels

Incorporation of all three wells into the kinetic model requires the solution of a system of three linear differential equations:

$$\frac{d[\mathbf{1}]}{dt} = (-k_1 - k_2)[\mathbf{1}] + k_{-2}[\mathbf{2}] = a_1[\mathbf{1}] + b_1[\mathbf{2}],$$

$$\frac{d[\mathbf{2}]}{dt} = k_2[\mathbf{1}] + (-k_{-2} - k_5 - k_3)[\mathbf{2}] + k_{-3}[\mathbf{3}] = a_2[\mathbf{1}] + b_2[\mathbf{2}] + c_2[\mathbf{3}],$$

$$\frac{d[\mathbf{3}]}{dt} = k_3[\mathbf{2}] + (-k_{-3} - k_4)[\mathbf{3}] = b_3[\mathbf{2}] + c_3[\mathbf{3}]$$

The resulting matrix:

$$\begin{bmatrix} \lambda + a_1 & b_1 & 0 \\ a_2 & \lambda + b_2 & c_2 \\ 0 & b_3 & \lambda + c_3 \end{bmatrix} \begin{pmatrix} \alpha \\ \beta \\ \delta \end{pmatrix} = \begin{pmatrix} 0 \\ 0 \\ 0 \end{pmatrix}$$

nominally results in a cubic polynomial that yields three roots (eigenvalues) λ_1, λ_2 and λ_3. Each of these three roots is associated with an eigenvector:

$$[\mathbf{1}] = c_1\alpha_1 e^{-\lambda_1 t} + c_2\alpha_2 e^{-\lambda_2 t} + c_3\alpha_3 e^{-\lambda_3 t},$$
$$[\mathbf{2}] = c_1\beta_1 e^{-\lambda_1 t} + c_2\beta_2 e^{-\lambda_2 t} + c_3\beta_3 e^{-\lambda_3 t},$$
$$[\mathbf{3}] = c_1\delta_1 e^{-\lambda_1 t} + c_2\delta_2 e^{-\lambda_2 t} + c_3\delta_3 e^{-\lambda_3 t}$$

The values for α, β and δ can be solved at each internal energy. It turns out that over the energy range probed in the TPEPICO experiment, the values of the eigenvectors are fairly constant; if the mid-point in the energy range is taken as a reference point, they are:

$$\begin{bmatrix} -0.707 & 1 & -0.550 \\ 0.707 & 0.062 & -0.032 \\ 0 & 0.002 & 0.835 \end{bmatrix}$$

which can be normalized with respect to β:

$$\begin{bmatrix} -1 & 16.10 & 17.35 \\ 1 & 1 & 1 \\ 0 & 0.03 & -26.32 \end{bmatrix}$$

The coefficients c_1, c_2 and c_3 can be determined from initial conditions ($[\mathbf{2}]_{t=0} = 0$ and $[\mathbf{3}]_{t=0} = 0$), and setting c_1 arbitrarily to **1**:

$$c_1 = 1, \qquad c_2 = -1, \qquad c_3 = -0.0011$$

The rate constants for the three exponential decay rates are given by:

$$k_a = 16.096k_1 + 0.03k_4 + k_5,$$
$$k_b = 0.02k_1 + 0.03k_4 + 0.0011k_5,$$
$$k_c = k_1 + k_5$$

where k_c is the rate constant corresponding to the reaction having the fastest rate (largest eigenvalue) and will only contribute near $t = 0$. Of k_a and k_b (Fig. 4) it is apparent only k_a represents the experimental data. The fraction of ions undergoing loss via k_b must be small. From the discussion presented for the two-well model it is likely that this channel involves the dissociation of ion **3**. The results for the two- and three-well models agree over the energy range of the experimental data but diverge at lower internal energies. This is due to the relative magnitudes of k_3 and k_5. At low internal energies k_3 is greater than k_5 (Fig. 3) and so the dissociation rate constant is reduced by the reversible isomerization of ion **2** to **3**. Above 1.01 eV dissociation of ion **2** out competes isomerization to ion **3** and the system behaves more like the two-well model.

The three-well potential model based on the B3-LYP/6-311++G(3df,2p)//B3-LYP/6-31+G(d) calculations is in excellent agreement with the experimental data. The relative amounts of the two radicals produced will primarily be governed by the relative magnitudes of the two rate constants k_1 and k_5. Over the internal energy range probed in the TPEPICO study this ratio k_5/k_1 varies from 7000 at 0.95 eV internal energy of **1** to 28 at 1.2 eV, and so it is the carbon-centered radical that is primarily formed in the experiment. It should be noted that the calculated observed rate constant is strongly dependent on the energetics of the surface. A difference of 10 kJ mol^{-1} in the dissociation energy of **1** results in a discrepancy between the calculated and the experimental rate constants greater than the experimental uncertainty.

4. Conclusion

The dissociative photoionization of the dimers of dimethylamine has been modeled with density functional theory calculations of the minimum energy reaction pathways of the dimer ion. The calculations predict that there are three stable equilibrium species on the potential energy surface which are accessible during the dissociation of the dimer ions to form protonated dimethylamine and a free radical (which can be either the nitrogen-centered $(CH_3)_2N^{\bullet}$ radical or the carbon-centered $CH_3NHCH_2^{\bullet}$ radical). The dissociation kinetics have been estimated using RRKM theory based on two-well and three-well models for the surface. The calculated observed rate constants for both models agree very well with experimental data obtained for the dissociation by Mayer et al. [11].

Acknowledgements

P.M. Mayer thanks the Natural Sciences and Engineering Research Council of Canada for continued funding, and the University of Ottawa for a grant towards the purchase of the computer workstation. P.M. Mayer also thanks the University of Montreal ESI Computing Center and the Queen's University HPCVL for generous donations of cpu time.

References

[1] P. Kebarle, in: J.M. Farrar, W.H. Saunders (Eds.), Techniques for the Study of Ion–Molecule Reactions, Vol. 20, Wiley-Interscience, New York, 1988, 221 pp.
[2] M. Meot-Ner, J. Am. Chem. Soc. 106 (1984) 1265.
[3] K. Hiraoka, H. Takimoto, S. Yamabe, J. Phys. Chem. 90 (1986) 5910.

[4] A.W. Castleman, S. Wei, Annu. Rev. Phys. Chem. 45 (1994) 685.
[5] A.W. Castleman, K.H. Bowen, J. Phys. Chem. 100 (1996) 12911.
[6] D. Smith, P. Spanel, Mass Spectrom. Rev. 14 (1995) 255.
[7] J.E. Szulejko, T.B. McMahon, Org. Mass Spectrom. 28 (1993) 1009.
[8] V. Aviyente, M. Iraqi, T. Peres, C. Lifshitz, J. Am. Soc. Mass Spectrom. 2 (1991) 113.
[9] H.E. Audier, C. Monteiro, P. Mourgues, D. Robin, Rapid Commun. Mass Spectrom. 3 (1989) 84.
[10] K.K. Matthews, N.G. Adams, N.D. Fisher, J. Phys. Chem. A101 (1997) 2841.
[11] P.M. Mayer, J.W. Keister, T. Baer, M. Evans, C.Y. Ng, C.-W. Hsu, J. Phys. Chem. A101 (1997) 1270.
[12] P.M. Mayer, J. Phys. Chem. A103 (1999) 3687.
[13] T.D. Fridgen, J.D. Keller, T.B. McMahon, J. Phys. Chem. A105 (2001) 3816.
[14] R.A. Ochran, A. Annamalai, P.M. Mayer, J. Phys. Chem. A104 (2000) 8505.
[15] R.A. Ochran, P.M. Mayer, Eur. Mass Spectrom. 7 (2001) 267–277.
[16] K. Raghavachari, J. Chandrasekhar, R.C. Burnier, J. Am. Chem. Soc. 106 (1984) 3124.
[17] J.C. Sheldon, G.J. Currie, J.H. Bowie, J. Chem. Soc. Perkin Trans. II (1986) 941.
[18] W. Koch, M.C. Holthausen, A Chemist's Guide to Density Functional Theory, Wiley-VCH, New York, 2000.
[19] M.J. Frisch, G.W. Trucks, H.B. Schlegel, G.E. Scuseria, M.A. Robb, J.R. Cheeseman, V.G. Zakrzewski, J.A. Montgomery, R.E. Stratmann, J.C. Burant, S. Dapprich, J.M. Millam, A.D. Daniels, K.N. Kudin, M.C. Strain, O. Farkas, J. Tomasi, V. Barone, M. Cossi, R. Cammi, B. Mennucci, C. Pomelli, C. Adamo, S. Clifford, J. Ochterski, G.A. Petersson, P.Y. Ayala, Q. Cui, K. Morokuma, D.K. Malick, A.D. Rabuck, K. Raghavachari, J.B. Foresman, J. Cioslowski, J.V. Ortiz, A.G. Baboul, B.B. Stefanov, G. Liu, A. Liashenko, P. Piskorz, I. Komaromi, R. Gomperts, R.L. Martin, D.J. Fox, T. Keith, M.A. Al-Laham, C.Y. Peng, A. Nanayakkara, C. Gonzalez, M. Challacombe, P.M.W. Gill, B. Johnson, W. Chen, M.W. Wong, J.L. Andres, C. Gonzalez, M. Head-Gordon, E.S. Replogle, J.A. Pople. Gaussian 98, Rev A.7; Gaussian, Inc.: Pittsburgh, PA, 1998.
[20] A.P. Scott, L. Radom, J. Phys. Chem. 100 (1996) 16502.
[21] P.M. Mayer, C.J. Parkinson, D.M. Smith, L. Radom, J. Chem. Phys. 108 (1998) 604.
[22] P.M. Mayer, J. Chem. Phys. 110 (1999) 7779.
[23] P.M. Mayer, J. Phys. Chem. A103 (1999) 5905.
[24] P.M. Mayer, Chem. Phys. Lett. 314 (1999) 311.
[25] M.J. Tubergen, R.L. Kuczkowski, J. Chem. Phys. 100 (1994) 3377.
[26] T. Beyer, D.R. Swinehart, ACM Commun. 16 (1973) 379.
[27] T. Baer, W.L. Hase, Unimolecular Reaction Dynamics, Theory and Experiments, Oxford University Press, New York, 1996.
[28] T. Baer, W.A. Brand, T.L. Bunn, J.J. Butler, Faraday Discuss. Chem. Soc. 75 (1983) 45.
[29] P.M. Mayer, T. Baer, J. Phys. Chem. 100 (1996) 14949.
[30] O.A. Mazyar, P.M. Mayer, T. Baer, Int. J. Mass Spectrom. Ion Proc. 167/168 (1997) 389.